BBA Clinical 7 (2017) 1–7

Contents lists available at ScienceDirect

BBA Clinical

journal homepage: www.elsevier.com/locate/bbaclin

A novel dominant D109A *CRYAB* mutation in a family with myofibrillar myopathy affects αB-crystallin structure

Jakub P. Fichna [a,*,1], Anna Potulska-Chromik [b,1], Przemysław Miszta [c,1], Maria Jolanta Redowicz [d], Anna M. Kaminska [b], Cezary Zekanowski [a,*], Sławomir Filipek [c]

[a] Laboratory of Neurogenetics, Department of Neurodegenerative Disorders, Mossakowski Medical Research Center, Polish Academy of Sciences, 02-106 Warszawa, 5 Pawinskiego St., Poland
[b] Department of Neurology, Medical University of Warsaw, 1a Banacha St., 02-097 Warsaw, Poland
[c] Faculty of Chemistry and Biological and Chemical Research Centre, University of Warsaw, 1 Pasteur St., 02-093 Warsaw, Poland
[d] Laboratory of Molecular Basis of Cell Motility, Department of Biochemistry, Nencki Institute of Experimental Biology, 3 Pasteur St., 02-093 Warsaw, Poland

ARTICLE INFO

Article history:
Received 8 September 2016
Received in revised form 9 November 2016
Accepted 10 November 2016
Available online 11 November 2016

Keywords:
CRYAB
HSPB5
Myofibrillar myopathy
Mutation
Molecular dynamics
Bioinformatics

ABSTRACT

Myofibrillar myopathy (MFM) is a group of inherited muscular disorders characterized by myofibrils dissolution and abnormal accumulation of degradation products. So far causative mutations have been identified in nine genes encoding Z-disk proteins, including αB-crystallin (CRYAB), a small heat shock protein (also called HSPB5). Here, we report a case study of a 63-year-old Polish female with a progressive lower limb weakness and muscle biopsy suggesting a myofibrillar myopathy, and extra-muscular multisystemic involvement, including cataract and cardiomiopathy. Five members of the proband's family presented similar symptoms. Whole exome sequencing followed by bioinformatic analysis revealed a novel D109A mutation in *CRYAB* associated with the disease. Molecular modeling in accordance with muscle biopsy microscopic analyses predicted that D109A mutation influence both structure and function of CRYAB due to decreased stability of oligomers leading to aggregate formation. In consequence disrupted sarcomere cytoskeleton organization might lead to muscle pathology. We also suggest that mutated RQDE sequence of CRYAB could impair CRYAB chaperone-like activity and promote aggregation of lens crystallins.

1. Introduction

Myofibrillar myopathy (MFM) is a clinically and genetically heterogeneous group of disorders characterized by myofibrillar disorganization and the presence of ectopic protein aggregates in skeletal muscle. The dissolution of myofibrils commences at the Z-disk. Abnormal expression of desmin (*DES*), myotilin (*MYOT*), αB-crystallin (*CRYAB* or *HSPB5*) and dystrophin (*DMD*) results in accumulation of degraded filamentous material in various patterns mostly in myofibril-free fiber regions around nuclei and under the sarcolemma. Membranous organelles are dislocated and their degradation in autophagic vacuoles can be also observed [1].

The clinical features of MFM are diverse. Patients usually present with slowly progressive muscle weakness that often begins in distal muscles and spreads proximally, but an early limb-girdle involvement can also occur. Cardiomyopathy is an associated symptom in 15–30% of cases [2]. The patients may also display remarkably different clinical manifestations and extra-muscular involvement, including autosomal dominant congenital posterior pole cataract (CPPC) in some families with neither cardiac nor muscular phenotype reported [3]. The age at onset ranges from infancy to the eighth decade of life, however, the majority of MFM begins in the fourth and fifth decades [4]. Due to the associated phenotypic features, and pathomorphological heterogeneity, the differential diagnosis between MFM and other late-onset myopathies with a predominantly distal distribution presents a clinical challenge.

A growing number of genes have been associated with MFM pathogenesis, causing subtypes of the disease [1]. So far nine MFM-causing genes encoding Z-disc associated proteins have been identified: *DES*, *CRYAB*, *MYOT*, Z band alternatively spliced PDZ-containing protein (*ZASP*), filamin C (*FLNC*), Bcl2-associated athanogene-3 (*BAG3*), four-and-a-half LIM protein-1 (*FHL1*), titin (*TTN*) and sarcomeric actin (*ACTA1*) (see [5] for review). MFM is usually transmitted in an autosomal dominant manner, however, autosomal recessive or X-linked MFM forms have also been described [6]. So far thirteen different *CRYAB* mutations were identified not only in isolated cases of MFM, but also in association with congenital cataract, cardiomyopathy and multisystemic phenotypes involving some or all of the above traits [7–9].

* Corresponding authors at: Laboratory of Neurogenetics, Department of Neurodegenerative Disorders, Mossakowski Medical Research Centre, Polish Academy of Sciences, 5 Pawinskiego St., 02-106 Warsaw, Poland.
E-mail addresses: jfichna@imdik.pan.pl (J.P. Fichna), c.zekanowski@imdik.pan.pl (C. Zekanowski).
[1] These authors equally contributed to the manuscript.

http://dx.doi.org/10.1016/j.bbacli.2016.11.004

The *CRYAB* gene maps to 11q23.1, comprises 3 exons spanning 3.2 kb, and encodes a 175-amino-acid protein with a molecular mass of ~20 kD [10]. The CRYAB protein (also called HSPB5) belongs to the ATP-independent HSPB family (small HSP), characterized by a conserved α-crystalline domain [11]. It was initially identified as one of the structural proteins of the eye lens, however, it is widely expressed in many tissues and organs, including skeletal and cardiac muscle. *CRYAB* upregulation has been linked with a variety of diseases depending on the tissue [12,13]. It is involved in many processes including prevention of abnormal folding of other proteins, cytoskeletal formation, apoptosis inhibition, and modulation of membrane fluidity [14]. In the muscle CRYAB functions as a chaperone in cytoskeletal intermediate filament assembly and stabilization [15–17]. In addition, CRYAB plays a role in the mammalian RNAi/microRNA pathway, modulating the Ago2/RISC activity and as a result cellular homeostasis in the skeletal muscle [18].

Cells expressing mutated *CRYAB* are characterized by protein aggregates of primarily the mutant CRYAB. HSPB family members form homo- and hetero-oligomeric complexes with other HSPBs, playing a key role in substrate recognition and chaperoning functions, resulting in differential clinical manifestation of various *CRYAB* mutations [19]. It remains unresolved whether aggregates of the CRYAB itself are associated with a gain-of-toxic mechanisms or loss of function.

Here, we report the first Polish female patient with MFM clinical diagnosis and a novel dominant *CRYAB* mutation, and we propose a model presenting the deleterious effect of the mutation on the protein structure and function.

2. Materials and methods

2.1. Genetic analyses

DNA was extracted from the peripheral blood of the proband using standard methods. Whole exome sequencing (WES) was performed commercially at the BGI Tech Solutions (Hong Kong) using SureSelect Human All Exon v5 + UTR enrichment kit and paired-end 100 nt sequencing on the Illumina HiSeq2000 platform. Fastq read files were generated from the sequencing platform via the Illumina pipeline. Adapter sequences in the raw data were removed and low quality reads with low base quality were discarded. In total, 240.451.900 “clean” paired-end reads were aligned to the human hg19 reference genome using Burrows-Wheeler Alignment (BWA) package [20]. Duplicate reads were removed with Picard and base quality Phred scores were recalibrated using GATK's covariance recalibration [21]. The 15 GB of aligned sequence data resulted in 99× median coverage of the target capture regions with 99.6% of target bases covered at least 10×. Alignments were viewed with Integrative Genomics Viewer [22]. SNP and indel variants were called using the GATK Unified Genotyper. Annovar was used for initial variant annotation [23] with further annotation, filtering and analysis performed on Galaxy platform (on PL-Grid Infrastructure). Selected mutations were confirmed using a direct fluorescence-based sequencing (ABI 3130 Genetic Analyzer, Applied Biosystems, USA).

2.2. Muscle biopsy

The open muscle biopsy of the proband's biceps brachii was performed, and the muscle specimen was processed for further analyses.

2.3. Light and fluorescence microscopy

Histological and histochemical evaluation was performed using a routine battery of methods. Immunohistochemistry was performed using rabbit polyclonal anti-CRYAB antibody (Medac GMBH, Germany) at 1:100 dilution.

2.4. Electron microscopy analysis of the muscle biopsy

Analysis was performed using standard methods. For electron microscopy analysis, a fragment of the muscle specimen was fixed in glutaraldehyde, post fixed in osmium tetroxide and then embedded in Spurr embedding medium (Electron Microscopy Sciences, USA). Ultrathin sections of the selected areas were stained with uranyl acetate and counterstained with lead citrate. The samples were viewed using a JEM 1200 EX2 electron microscope.

2.5. Molecular modeling

2.5.1. System preparation

The 24-mer oligomeric structure of human CRYAB was downloaded from the Protein Data Bank (PDB code 2YGD) [24]. Only first six monomers (chains A to F), which create the symmetrical circular structure, were taken for the simulation. Three different *CRYAB* variants were investigated: the native protein, novel mutation D109A and previously described mutation affecting the same residue: D109H. The mutated histidine was used in neutral form as it was assumed for other histidine residues in the oligomer. D109 residue was mutated in all six monomers in the oligomer. All energy minimizations, equilibrations and molecular dynamics (MD) simulations were carried out in the NAMD program version 2.10 [25] using the CHARMM27 for protein force field [26]. Additionally, instead of explicit water molecules, the implicit solvent method was applied.

2.5.2. Molecular Dynamics (MD) simulations

Each structure of oligomeric CRYAB was initially subjected to 10,000 steps of energy minimization and then 100 ns MD equilibration with increasing temperature from 20 K to 298 K in the first steps of MD: 1 K per 1 step. The MD simulations were performed using Langevin (stochastic) dynamics [27], which is a default in the NAMD program for implicit solvent method. In Langevin dynamics the molecules interact with a stochastic heat bath via random and dissipative forces. The friction coefficient of 50 ps^{-1} was used and temperature was set to 298 K. For the van der Waals and electrostatic interactions a cutoff of 14 Å was used with a switching function for soft dampening the remaining interactions. For each investigated system 100 ns MD simulation was performed with a time step of 1 fs. All figures of molecular structures were created using the VMD program (v.1.9.2) [28].

2.6. Ethics statement

Written consent was obtained from all patients and healthy individuals according to the Declaration of Helsinki. The study was approved by the Ethics Committee of the Warsaw Medical University and the MSW Hospital (Warszawa, Poland) in compliance with the national legislation and the Code of Ethical Principles for Medical Research Involving Human Subjects of the World Medical Association.

3. Results

3.1. Case description

Proband (III.20; see Suppl. Fig. 1): a 63-year-old Caucasian female, with a positive family history of the disease. At 26 years, she developed progressive lower limb weakness pronounced mainly distally (dropping feet), followed by difficulty in climbing stairs and frequent falls. Further observation (to date) revealed a constant slow progression. At the age of 47 the patient fell and broke her vertebral column at the level Th12 and L1. She stopped walking unsupported at the age of 55 years and began to be wheelchair-dependent. Her father, two paternal brothers and two paternal sisters (Fig. 1; for details of their medical records see supporting information) presented with similar symptoms.

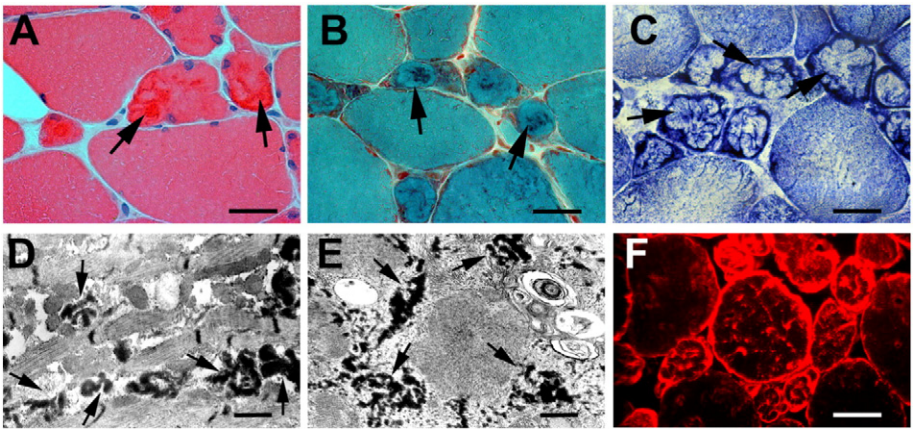

Fig. 1. Analysis of the proband's muscle. A) Hematoxylin/eosin (HE) staining; B) Trichrome staining; C) Succinate dehydrogenase (SDH) staining; D) and E) Electron micrographs; and F) Immunostaining with anti-CRYAB antibody. Arrows in A) and B) point at the dark material; in C) point to lobulated fibers, and in D) and E) point to electron dense material. Bars: 10 μm in A–C and F, and 500 nm in D and E.

Neurological examinations of the proband revealed nasal speech, dysphagia, high arched palate, significant weakness and wasting of the upper limbs muscles, mostly pronounced in the proximal part of the limbs. Deep tendon reflexes were diminished in the upper and lower limbs. In the lower limbs patient was able to move only her feet. At the age of 56 years. chronic respiratory failure was diagnosed and the patient is (to date) on nocturnal noninvasive ventilation. Chronic cardiac insufficiency was diagnosed at the age of 55 years. due to dilated cardiomiopathy. The biochemical and hematological parameters of the proband remains within normal limits except of elevation of serum creatine-kinase (CK) activity (81.39 IU).

The electromyogram (EMG), performed when the proband was 31 years old, showed myopathic features (decreased duration and size index of the motor unit action potentials, MUAP) were observed for the right first interosseous muscle as well as right vastus lateralis and tibialis anterior muscles. At the age of 52 years the results of the nerve conduction study were no different from normal subjects except for a decrease of M-response amplitude to right peroneal nerve stimulation (presumably due to atrophy of the muscle). CT scans of the lower limbs indicated complete muscle atrophy of both shins and thighs with relatively sparing of the adductors magnus and semimembranosus muscles.

In addition, among other symptoms the proband presented with cataract in the right eye, which was identified and operated at the age of 35 years. Fundus of the eye was normal. At that time, myotonic dystrophy was also suspected due to cataract and myopathy.

The morphological analysis of the muscle biopsy performed at 51 years showed moderate myopathic changes (see Fig. 1). The fascicular architecture of the muscle revealed a marked variability in fiber size and shape, with atrophy of some fibres, partially preserved as “nuclear clumps” (Fig. 1A-C). The presence of dark red material in hematoxylin/eosin (HE) staining (Fig. 1A, arrows) and dark blue material in trichrome staining (Fig. 1B, arrows) as well as of lobulated fibers in succinate dehydrogenase (SDH) staining (Fig. 1C, arrows) was observed.

Electron microscopy revealed profound changes in the fiber and sarcomer organization (Fig. 1D-E). In particular, disorganization of the sarcomers as well as the presence of electron dense material (Fig. 1D, arrows) was observed in the longitudinal sections. In addition, myelin figures and vacuolar structures were visible in the transverse sections, along with the electron dense material (Fig. 1E, arrows).

Immunohistochemistry using an anti-CRYAB antibody showed that unlike in normal muscle which show faint CRYAB positivity, especially at myomuscular and myotendinous junctions [29] but not at neuromuscular junctions CRYAB was located in aggregate-like structures distributed not only beneath the sarcolemma but also within the fibers, both in atrophic and normal-sized ones (Fig. 1F).

3.1.1. Proband's relatives

Proband's father (II.11, see Suppl. Fig. 1) developed progressive lower limb weakness distal > proximal (dropping feet) followed by difficulty climbing stairs at the age of 48 years. Neurological examination performed one year later revealed distal weakness and wasting of the upper and lower limbs. Deep tendon reflexes were diminished in the upper and lower limbs. Condition of the patient steadily deteriorated. The patient died at the age of 69 years.

Proband's uncle (II.3, see Suppl. Fig. 1) developed slowly progressive distal weakness followed by proximal paresis at around 50 years of age. Cataract in both eyes was found and surgery was performed at the age of 53.

Proband's aunt (II.8, see Suppl. Fig. 1) developed muscle weakness from distal part of the lower limbs (dropping feet) at around 40 years of age. She experienced cataract of both eyes and had surgery at the age of 45. Neurological examination performed at the age of 61 years revealed significant weakness and wasting of the upper as well as lower limbs muscles.

Moreover, the second proband's uncle (II.1) and aunt (II.10) showed similar symptoms, however, no detailed medical history is available. For a detailed comparison of the clinical characteristic of the affected family members of the proband see Suppl. Table 1.

3.2. Genetic analyses

Whole exome sequencing identified 126.804 SNPs and 23.284 InDels, of which 76.101 and 14.815 respectively were off target (defined as intergenic or intronic, but not affecting splice sites) and removed from further consideration.

Further filtering was based on allele frequency in ExAC database (<3% for variants in genes already associated with MFM, and <1% for variants in other genes), and predicted pathogenicity (predicted pathogenic by at least one out of Mutation Taster, PolyPhen2, and SIFT software). In total, 1.674 genes were further analyzed. Prioritization was based on the predicted effect, with truncating and elongating variants being evaluated more carefully, on predicted pathogenicity, and on known association with myopathic phenotypes. Independent additional analysis was performed with Exomiser2, PhenIX and Exome walker, prioritising variants based on their potential association with the Human Phenotype Ontology term “myopathy” and based on random-walk analysis of protein interaction networks [30]. As a result of each

Table 1
Putative causative or phenotype-modifying genetic variants identified in the proband. SNVs and indels that passed initial filtering (Phred quality score of at least 30, missense/nonsense/indel mutations for coding sequences = MODERATE or HIGH impact) and filtering for "muscle weakness" in HPO terms related to the gene. cDNA and protein alterations are reported in the following transcripts: ENST00000460472 (*TTN*), ENST00000533475 (CRYAB), ENST00000337435 (NIPA1), ENST00000261866 (SPG11).

Chr	Position	dbSNP	REF	ALT	Type	Impact	Gene	HGVS.c	HGVS.p	Genotype	ExAC MAF	In lab MAF	Mutation count
2	179597600	rs72648937	C	T	Missense	MODERATE	TTN	c.15352G > A	p.Val5118Met	het	0.00564	0.021	4/188
2	179599667	rs72648927	G	C	Missense	MODERATE	TTN	c.14033C > G	p.Pro4678Arg	het	0.01062	0.021	4/188
4	184596309	rs140871779	CT	C	Intronic/splice	LOW	TRAPPC11			het	0.1467	0.064	12/188
11	111779690	.	T	G	Missense/splice	MODERATE	CRYAB	c.326A > C	p.Asp109Ala	het	–	0.005	1/188
14	68194090	rs58392863	AG	A	Downstream	LOW	ZFYVE26			het	–	0.016	3/188
14	68233171	.	G	A	Intronic/splice	LOW	ZFYVE26			het	–	0.005	1/188
15	23086364	rs531550505	GGCC	G	Inframe deletion	MODERATE	NIPA1	c.45_47delGGC	p.Ala16del	het	0.01442	0.149	28/188
15	44907562	rs111347025	T	C	Missense/splice	MODERATE	SPG11	c.3037A > G	p.Lys1013Glu	het	0.00993	0.011	2/188

Chr: chromosome; Position: genomic position within a chromosome; dbSNP: record in Database of Single Nucleotide Polymorphism; REF: reference base; ALT: alternative base (base change); Type: mutation type; Impact: simple estimation of putative impact by snpeff; Gene: gene symbol; HGVS.c: coding RNA sequence variant; HGVS.p: protein sequence variant; genotype: zygosity; EXAC MAF: minor allele frequency in EXAC database; in-house MAF: minor allele frequency within 94 samples in our in-house database; mutation count: number of alleles with a mutation in our in house database.

of the above-described approaches, the identified *CRYAB* D109A mutation ranked in top places (Table 1).

CRYAB D109A mutation is a novel mutation, not registered in the ExAC database, despite over 120.000 sequenced *CRYAB* alleles. D109A mutation is predicted to be causative by the MutationTaster2, Polyphen2 and SIFT algorithms. According to the SIFT effect protein function score for D109A is 0.00, where <0.05 means deleterious. Likewise, Polyphen2 suggested that D109A substitution is damaging to the protein structure with a score of 1.00. D109A mutation is located within the fourth β strand of the conserved Alpha-Crystallin Domain (ACD) that consists of seven β strands and is involved in the protein dimerization. The other domains flanking ACD, i.e. hydrophobic and flexible N-terminal (NTR) and hydrophilic C-terminal (CTR) contribute to regulation of the protein activity and the solubility of the oligomers, respectively [31] (see Fig. 2). As shown in Table 2, aspartic acid residue at position 109 is present not only in the mammalian but also in the invertebrate *CRYAB* homologues.

The D109A mutation was confirmed using a direct fluorescence-based sequencing in the proband. Every affected family members that was tested (III:20, II:3, II:8) harbored the mutation, and it was not present in the healthy family member (IV:7). The mutation was also absent in 86 ethnically matched exomes from our in-lab database.

3.3. Molecular modelling

CRYAB is composed mostly of β-sheets and forms a large oligomeric structure. For the purpose of this research a hexamer (1050 residues) taken from 24-mer structure was used (Fig. 2A). This approach was used to increase statistical probability of finding an influence of a single mutation on the whole oligomeric structure of CRYAB, since there are six mutations in the structure and additionally the β-barrel-like structure of hexamer can be more sensitive to the possible changes introduced by the mutation. Each monomer is composed of a double β-sheet (larger and smaller with three β-threads in each) in form of a

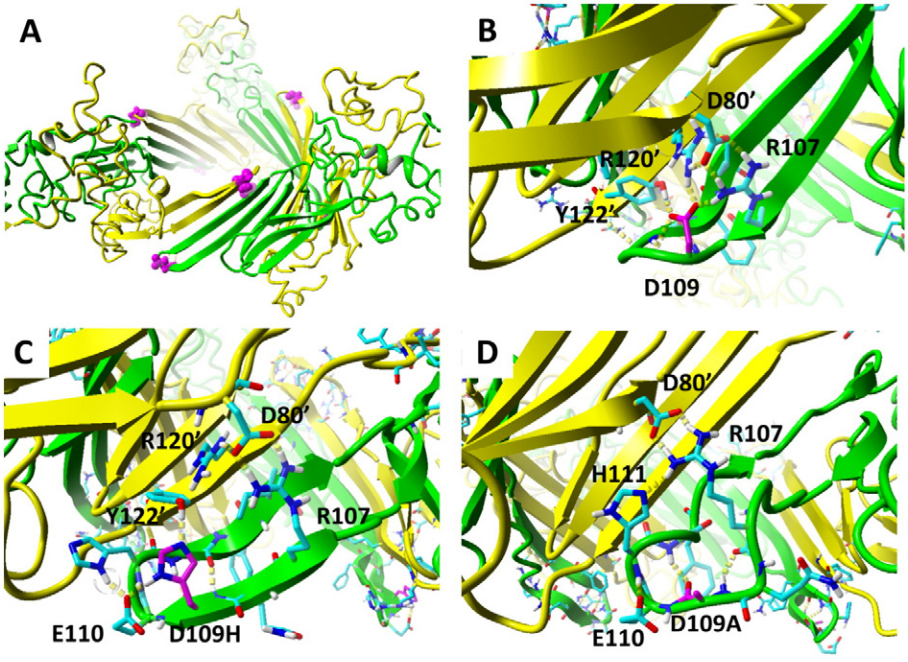

Fig. 2. Circular hexamer of CRYAB. A) WT crystal structure. The particular monomers are colored yellow and green, alternatively. D109 residue is colored in purple and shown as balls. B), C) and D) CRYAB oligomeric structure after 600 ns of MD simulation. D109 residue is labeled in purple. Prim marked positions in adjacent monomer (in yellow). The structures: WT, D109H, and D109A, respectively. Mutations rearrange the network of local interactions (D109A to the largest extent) which leads to destabilization (partial unfolding) of monomer-monomer interfaces and in consequence to decreased stability of the whole oligomer.

Table 2
Alignment of CRYAB amino acid sequence (*H. sapiens* positions: 98–120) with homologs' sequences. Aspertic acid residue affected in the proband and its evolutionary conserved homologs marked in red.

Species	Gene	aa position	Alignment
H. sapiens	ENST00000533475	109	IEVHGKHEERQDEHGFISREFHR
P. troglodytes	ENSPTRG00000004274	109	IEVHGKHEERQDEHGFISREFHR
M. mulatta	ENSMMUG00000022133	109	IEVHGKHEERQDEHGFISREFHR
F. catus	ENSFCAG00000015671	109	IEVHGKHEERQDEHGFISREFHR
M. musculus	ENSMUSG00000032060	109	IEVHGKHEERQDEHGFISREFHR
G. gallus	ENSGALG00000007945	108	IE**I**HGKHEERQDEHGF**I**A**R**EF**S**R
D. rerio	ENSDARG00000052447	98	IE**I**H**A**KHE**D**RQ**D**G**H**GF**V**SREF**L**R
D. melanogaster	FBgn0001229	115	I**VV**EGKHEER**E**D**D**HG**HV**SR**H**F**V**R
C. elegans	F52E1.7	91	**LII**EGKH**N**E**K**T**D**K**Y**G**QV**ER**H**F**V**R
X. tropicalis	ENSXETG00000010174	108	IE**I**HG**T**HEERQDEHG**YV**SR**D**F**Q**R

sandwich and a larger β-sheet of all monomers contributes to a central ring of oligomer. The primary, longer interface between monomers (residues 112–122) forms very strong intermolecular β-sheet, while the secondary interface in the β-barrel (residues 91–94) contains a large gap between β-threads so the intermolecular β-sheet is weak. This contact is mostly maintained by extended coiled-coil interactions by the rest of CRYAB structure.

In a wild type (WT) protein, the aspartic acid residue 109 (D109) forms hydrogen bonds and ionic interactions with adjacent residues, namely arginine 107 (R107) from the same monomer as well as with arginine 120 (R120′) and tyrosine 122 (Y122′) on the adjacent monomer. The interaction of R107 and R120 is stabilized by D80' from adjacent monomer, which closely interacts with both arginine residues (Fig. 2B). The other causative mutation, D109H, is predicted to maintain a hydrogen bond to Y122 but not ionic interactions with arginine residues R107 and R120. Instead, it frequently forms a hydrogen bond with adjacent residue E110 from the same monomer (Fig. 2C). The ionic interactions between residues R107-D80′-R120′ are preserved however lack the stabilizing negative charge from D109. The whole structure of the oligomer is less stable than WT since some of the β-sheets are unfolded. The identified mutation, D109A, is predicted to lead to additional unfolding of β-sheets. Number of residues participating in b-sheets, which form the core of CRYAB, diminished by >10% compared to reduction by 4% for D109H. In consequence, the contact between monomers decreases, making the oligomer less stable. Since a side chain of A109 cannot participate in the hydrogen bonds as well as in ionic interactions with any adjacent residues, the triple interaction R107-D80′-R120′ is less stable. Hence, in some interfaces between monomers a disintegration of the triple interaction into two pair interactions (E106-R107 and D80′-R120′) was observed. As a result, CRYAB monomers lose the contact with each other (Fig. 2D). Not all interfaces change to the same extent in the same time as this is a statistical process, so it seems that changes start in one particular interface and then, possibly due to a resonance effect in the β-barrel, they are distributed to other interfaces via weakening them.

4. Discussion

We have presented a case of the first Polish patient with a clinical and morphological diagnosis of MFM, carrying a novel dominant mutation in the *CRYAB* gene. Using bioinformatic tools, we propose a putative model presenting effects of the D109A mutation on the protein structure and function.

First, using WES approach we have identified in the proband eight putative causative or phenotype-modifying genetic variants. SNVs and indels that passed initial filtering are listed in Table 1. Out of these variants only D109A mutation matches the clinical and morphological phenotype of the proband characteristic for crystallinopathies described so far [32]. Variants identified within *TTN* (affecting Ig-like domains 28 and 31) though predicted to have a moderate impact do not match the symptoms, as TTN-causative myopathy are known to have early-late adulthood onset and early respiratory insufficiency associated with the titin-associated subtype of MFM [32]. Also, the *TRAPPC11* variant does not seem to be pathogenic as mutations within this gene cause a myopathy with intellectual disability as well as with fatty liver and infantile cataract which are not the case here [33,34]. Variants identified in *ZFYVE26* also seem not to be pathogenic as known ZFYVE26 mutations are associated with complicated hereditary spastic paraparesis and autophagy [35]. The same is the case of *NIPA1* and *SPG11* variants, as abnormalities within both proteins are known to be associated with hereditary spastic paraplegia [36]. However, it is possible that aforementioned variants could affect the course of the disease, worsening the proband condition.

Most of the myopathy-associated mutations described so far (D109H, R120G, Q151X, G154S, P155Rfs9X, R157H) were found in the ACD [8]. Besides myopathy, mutations D109H, R120G and X176Wfs19X are so far the only ones associated with signs of cardiomyopathy and cataract or discrete lens opacities [7]. Other recessive (e.g. R11C, R12C, R56W), and dominant (R11H, P20R, P20S, R69C, D140N, K150Nfs34X, A171T) *CRYAB* mutations associated with congenital cataract were also described, uniformly scattered all over the coding sequence [37].

D109 residue is located in the core domain between β3 (75-83) and FISREFHR motif (113–120, see Table 2). D109 residue is adjacent to 113-120 sequence important for microtubule assembly and aggregation prevention [38].

The first identified mutation in this residue (D109H) is responsible for autosomal dominant multisystemic phenotype, not only with myopathic features, but also with cardiomyopathy and lens cataract [39]. Previously, it was shown that D109H mutant protein can enhance protein aggregation and cell apoptosis in the HeLa cells [40]. This explains well the mechanism of *CRYAB* mutations associated with myopathy and decreased lens transparency, and also the involvement of CRYAB expression in tauopathies [41]. In muscle, mutated CRYAB binds stronger to desmin and instead of facilitating formation of intermediate filament network, it promotes aggregation of both proteins [42]. In our study, such CRYAB stained large aggregates as well as desmin-derived electron dense material were found in the proband's muscle (see Fig. 1D-F).

Involvement of CRYAB in the regulation of intracellular apoptotic signals and inhibition of apoptosis through activation of Akt pathway and enhancing PI3K activity [43,44]; could also easily explain not only *CRYAB* mutations in myopathy [45], but also *CRYAB* overexpression in some types of cancer [46].

Previous reports on D109H and R120G mutations, both associated with a multisystemic phenotype, suggested that residues D109 and R120 interact with each other during dimerization of CRYAB [39]. For a better delineation of molecular interactions between the mutated residues and their immediate surrounding we performed molecular dynamics simulations.

We have shown in more detail that D109 is a part of a network of intramolecular interactions with residues within same monomer and adjacent monomers, strengthening the hexamer structure. The D109H mutation decreases the stability of oligomer since H109 interacts with less residues. Some of the β-sheets, which form the core of CRYAB, are unfolded. Likewise the D109A mutation cannot stabilize interaction with adjacent monomer of CRYAB and the β-sheets of this protein are even additionally unfolded, as compared to D109H. In consequence CRYAB monomers lose the contact with each other.

Our results are consistent with and strengthen the previously published results, showing that CRYAB interactions, also with a variety of target proteins, depend on weak non-covalent interplay between a number of bioactive sequences scattered all over the CRYAB sequence

and forming a network of highly sensitive areas for protein–protein interactions [47]. Interestingly, the mutated residue studied herein (D109) is located in the HGKHEERQDE sequence, which is one of the most effective inhibitors of amyloid-beta (Aβ) fibril formation [47–49]. This motif is located not in the monomer-monomer interface but in the second row (2nd β-thread in β-sheet). Since 3rd β-thread is about a half-length of previous ones, the whole motif is open to water solution and hence exposed to additional oligomerization. D109 is located at the end of 2nd β-thread close to β-turn linking to 1st β-thread. Therefore, the identified mutation D109A destabilizes not only the interface between monomers so the whole oligomer loses its stability, but also, due to the modified sequence motif, makes it more prone to fibril formation. This is particularly important, as the distal parts of this sequence (i.e.: HEER and RQDE) were shown to enhance fibril formation of Aβ [47–49]. As native CRYAB is protective against aggregation of lens crystallins in aging cataract, it could be speculated that D/A and D/H substitutions in position 109 diminish the native functional role of the whole HGKHEERQDE sequence [50]. These predictions were confirmed by immunostaining for CRYAB of the proband's biopsied muscle that showed the presence of large aggregate-like structures distributed not only at the fiber periphery but also within the fiber.

Therefore, we suggest two ways of explaining the pathogenic mechanism of the D109A mutation. First, the mutation may cause aggregation of other proteins including lens crystallins and muscular desmin via dominant negative effect on the chaperone function of oligomeric CRYAB complexes with other partners (including other HSPB family members), leading to insufficient prevention of aggregation of other proteins. Alternatively, the structural instability and propensity to aggregate of the mutated CRYAB itself results in gain-of-function i.e. formation of the visible CRYAB aggregates.

The molecular differences between both mutations (D109A and D109H) cannot be directly translated into differences in clinical phenotypes of affected individuals. It could be speculated that CRYAB oligomeric structures of diverged stability display disturbed interaction with the same protein partners, resulting in common clinical symptoms. The phenotypic diversity has been related to the different interactions between target proteins, including members of the HSPB family with individual CRYAB mutated residues impairing hetero-oligomeric complexes resulting in differently impaired chaperoning functions towards different substrates [51]. However, in the case of D109A mutation we observed a minor intrafamiliar variability in the clinical phenotype and the age of onset (30–50 years), however with homogenous dominant features involving muscular, cardiac and ocular systems.

In conclusion, this is a first report of a Polish patient presenting with crystallinopathy and multisystemic involvement. According to the cosegregation within a family and *in silico* analyses, the *CRYAB* D109A mutation may be assumed pathogenic [52]. Molecular modeling in accordance with muscle biopsy microscopic analyses and the clinical data predicted that D109A influence both structure and function of CRYAB due to decreased stability of oligomers leading to aggregate formation. In consequence disrupted sarcomere cytoskeleton organization might lead to muscle pathology. Additionally, impaired CRYAB chaperone-like activity due to mutated RQDE sequence, could promote aggregation of lens crystallins [50].

Supplementary data to this article can be found online at http://dx.doi.org/10.1016/j.bbacli.2016.11.004.

Transparency Document

The Transparency document associated with this article can be found, in online version.

Acknowledgements

This work was supported by a National Science Centre, Poland grant (NCN, 2012/05/D/NZ4/02978 to JPF, SF, AMK, PM, APC) and by the KNOW-MMRC project financed by the Ministry of Science and Higher Education (to JPF). The bioinformatics analysis (JPF) was partially supported by PL-Grid Infrastructure financed by the Ministry of Science and Higher Education and co-funded by the European Regional Development Fund as part of the Innovative Economy program. This work was also partially supported by a statutory grant to the Department of Neurology, Medical University of Warsaw from the Ministry of Science and Higher Education (APC, AMK). The funding bodies had no involvement in the experimental design, analysis, data interpretation and manuscript preparation.

References

[1] M. Olivé, R.A. Kley, L.G. Goldfarb, Myofibrillar myopathies: new developments, 2013. Opin. Neurol. 26 527–535, http://dx.doi.org/10.1097/WCO.0b013e328364d6b1.
[2] P. Pruszczyk, A. Kostera-Pruszczyk, A. Shatunov, B. Goudeau, A. Draminska, K. Takeda, N. Sambuughin, P. Vicart, S.V. Strelkov, L.G. Goldfarb, A. Kaminska, Restrictive cardiomyopathy with atrioventricular conduction block resulting from a desmin mutation, 2007. Int. J. Cardiol. 117 244–253, http://dx.doi.org/10.1016/j.ijcard.2006.05.019.
[3] J.J. van der Smagt, A. Vink, J.H. Kirkels, M. Nelen, H. ter Heide, M.M. Molenschot, R.A. Weger, P.A. Schellekens, J. Hoogendijk, D. Dooijes, Congenital posterior pole cataract and adult onset dilating cardiomyopathy: expanding the phenotype of αβ-crystallinopathies, 2014. Clin. Genet. 85 381–385, http://dx.doi.org/10.1111/cge.12169.
[4] R. Schröder, B. Schoser, Myofibrillar myopathies: a clinical and myopathological guide, 2009. Brain Pathol. 19 483–492, http://dx.doi.org/10.1111/j.1750-3639.2009.00289.x.
[5] A. Béhin, E. Salort-Campana, K. Wahbi, P. Richard, R.Y. Carlier, P. Carlier, P. Laforêt, T. Stojkovic, T. Maisonobe, A. Verschueren, J. Franques, S. Attarian, A. Maues de Paula, D. Figarella-Branger, H.M. Bécane, I. Nelson, D. Duboc, G. Bonne, P. Vicart, B. Udd, N. Romero, J. Pouget, B. Eymard, Myofibrillar myopathies: state of the art, present and future challenges, 2015. Rev. Neurol. (Paris) 171 715–729, http://dx.doi.org/10.1016/j.neurol.2015.06.002.
[6] K.Y. van Spaendonck-Zwarts, L. van Hessem, J.D. Jongbloed, H.E. de Walle, Y. Capetanaki, A.J. van der Kooi, I.M. van Langen, M.P. van den Berg, J.P. van Tintelen, Desmin-related myopathy, 2011. Clin. Genet. 80 354–366, http://dx.doi.org/10.1111/j.1399-0004.2010.01512.x.
[7] P. Vicart, A. Caron, P. Guicheney, Z. Li, M.C. Prevost, A. Faure, D. Chateau, F. Chapon, F. Tomé, J.M. Dupret, D. Paulin, M. Fardeau, A missense mutation in the alphaβ-crystallin chaperone gene causes a desmin-related myopathy, 1998. Nat. Genet. 20 92–95, http://dx.doi.org/10.1038/1765.
[8] X. Jiaox, S.Y. Khan, B. Irum, A.O. Khan, Q. Wang, F. Kabir, A.A. Khan, T. Husnain, J. Akram, S. Riazuddin, J.F. Hejtmancik, S.A. Riazuddin, Missense mutations in CRYAB are liable for recessive congenital cataracts, 2015. PLoS One 24 e0137973, http://dx.doi.org/10.1371/journal.pone.0137973.
[9] N. Inagaki, T. Hayashi, T. Arimura, Y. Koga, M. Takahashi, H. Shibata, K. Teraoka, T. Chikamori, A. Yamashina, A. Kimura, Alpha-β crystallin mutation in dilated cardiomyopathy, 2006. Biochem. Biophys. Res. Commun. 342 379–386, http://dx.doi.org/10.1016/j.bbrc.2006.01.154.
[10] R.A. Dubin, A. Ally, S. Chung, J. Piatigorsky, Human alpha-β-crystallin gene and preferential promoter function in lens, Genomics 7 (1990) 594–601 (PMID: 2387586).
[11] E. Basha, H. O'Neill, E. Vierling, Small heat shock proteins and α-crystallins: dynamic proteins with flexible functions, 2012. Trends Biochem. Sci. 37 106–117, http://dx.doi.org/10.1016/j.tibs.2011.11.005.
[12] Q.M. Shi, J. Luo, K. Wu, M. Yin, Y.R. Gu, X.G. Cheng, High level of αβ-crystallin contributes to the progression of osteosarcoma, 2016. Oncotarget 23 9007–9016, http://dx.doi.org/10.18632/oncotarget.6928;
H. Shinohara, Y. Inaguma, S. Goto, T. Inagaki, K. Kato, αβ crystallin and HSP28 are enhanced in the cerebral cortex of patients with Alzheimer's disease, 1993. J. Neurol. Sci. 119 203–208, http://dx.doi.org/10.1016/0022-510X(93)90135-L.
[13] Y. Liu, Q. Zhou, M. Tang, N. Fu, W. Shao, S. Zhang, Y. Yin, R. Zeng, X. Wang, G. Hu, J. Zhou, Upregulation of alphaβ-crystallin expression in the substantia nigra of patients with Parkinson's disease, 2015. Neurobiol. Aging 36 1686–1691, http://dx.doi.org/10.1016/j.neurobiolaging.2015.01.015.
[14] P.J. Muchowski, J.A. Bassuk, N.H. Lubsen, J.I. Clark, Human alphab-crystallin. Small heat shock protein and molecular chaperone, J. Biol. Chem. 272 (1997) 2578–2582 (PMID: 8999975).
[15] F. Bennardini, A. Wrzosek, M. Chiesi, αβ-crystallin in cardiac tissue: association with actin and desmin filaments, Circ. Res. 71 (1992) 288–294 (PMID: 1628387).
[16] I.D. Nicholl, R.A. Quinlan, Chaperone activity of α-crystallins modulates intermediate filament assembly, EMBO J. 13 (1994) 945–953 (PMID: 7906647).
[17] K. Wang, A. Spector, α-Crystallin stabilizes actin filaments and prevents cytochalasin-induced depolymerization in a phosphorylation-dependent manner, 1996. Eur. J. Biochem. 242 56–66, http://dx.doi.org/10.1111/j.1432-1033.1996.0056r.x.
[18] R.L. Neppl, M. Kataoka, D.Z. Wang, Crystallin-αβ regulates skeletal muscle homeostasis via modulation of argonaute2 activity, 2014. J. Biol. Chem. 289 17240–17248, http://dx.doi.org/10.1074/jbc.M114.549584.
[19] A.P. Arrigo, Human small heat shock proteins: protein interactomes of homo- and hetero-oligomeric complexes: an update, 2013. FEBS Lett. 587 1959–1969, http://dx.doi.org/10.1016/j.febslet.2013.05.011.
[20] H. Li, R. Durbin, Fast and accurate short read alignment with Burrows-Wheeler transform, 2009. Bioinformatics 25 1754–1760, http://dx.doi.org/10.1093/bioinformatics/btp324.

[21] A. McKenna, M. Hanna, E. Banks, A. Sivachenko, K. Cibulskis, A. Kernytsky, K. Garimella, D. Altshuler, S. Gabriel, M. Daly, M.A. DePristo, The Genome Analysis Toolkit: a MapReduce framework for analyzing next-generation DNA sequencing data, 2010. Genome Res. 20 1297–1303, http://dx.doi.org/10.1101/gr.107524.110.
[22] J.T. Robinson, H. Thorvaldsdóttir, W. Winckler, M. Guttman, E.S. Lander, G. Getz, J.P. Mesirov, Integrative genomics viewer, 2011. Nat. Biotechnol. 29 24–26, http://dx.doi.org/10.1093/bib/bbs017.
[23] K. Wang, M. Li, H. Hakonarson, ANNOVAR: functional annotation of genetic variants from high-throughput sequencing data, 2010. Nucleic Acids Res. 38 e164, http://dx.doi.org/10.1093/nar/gkq603.
[24] N. Braun, M. Zacharias, J. Peschek, A. Kastenmuller, J. Zou, M. Hanzlik, M. Haslbeck, J. Rappsilber, J. Buchner, S. Weinkauf, Multiple molecular architectures of the eye lens chaperone alphaB-crystallin elucidated by a triple hybrid approach, 2011. Proc. Natl. Acad. Sci. U. S. A. 108 20491–20496, http://dx.doi.org/10.1073/pnas.1111014108.
[25] J.C. Phillips, R. Braun, W. Wang, J. Gumbart, E. Tajkhorshid, E. Villa, C. Chipot, R.D. Skeel, L. Kale, K. Schulten, Scalable molecular dynamics with NAMD, 2005. J. Comput. Chem. 26 1781–1802, http://dx.doi.org/10.1002/jcc.20289.
[26] A.D. MacKerell, N. Banavali, N. Foloppe, Development and current status of the CHARMM force field for nucleic acids, 2001. Biopolymers 56 257–265, http://dx.doi.org/10.1002/1097-0282(2000)56:4<257::AID-BIP10029>3.0.CO;2-W.
[27] M. Toda, R. Kubo, N. Saitō, N. Hashitsume, Statistical Physics II: Nonequilibrium Statistical Mechanics, Springer, Berlin Heidelberg, 1992.
[28] W. Humphrey, A. Dalke, K. Schulten, VMD: visual molecular dynamics, J. Mol. Graph. 14 (1996) 33–38 (27-8, PMID: 8744570).
[29] B.L. Banwell, A.G. Engel, [Alpha]b-crystallin immunolocalization yields new insights into inclusion body myositis, 2000. Neurology 54 1033–1041, http://dx.doi.org/10.1212/WNL.54.5.1033.
[30] D. Smedley, P.N. Robinson, Phenotype-driven strategies for exome prioritization of human Mendelian disease genes, 2015. Genome Med. 7 81, http://dx.doi.org/10.1186/s13073-015-0199-2.
[31] M. Haslbeck, J. Peschek, J. Buchner, S. Weinkauf, Structure and function of α-crystallins: traversing from in vitro to in vivo, 2016. Biochim. Biophys. Acta 1860 (1 Pt B) 149–166, http://dx.doi.org/10.1016/j.bbagen.2015.06.008.
[32] R.A. Kley, M. Olivé, R. Schröder, New aspects of myofibrillar myopathies, Curr. Opin. Neurol. (Jul 8 2016) ([Epub ahead of print]; PMID: 27389816).
[33] N. Bögershausen, N. Shahrzad, J.X. Chong, J.C. von Kleist-Retzow, D. Stanga, Y. Li, F.P. Bernier, C.M. Loucks, R. Wirth, E.G. Puffenberger, R.A. Hegele, J. Schreml, G. Lapointe, K. Keupp, C.L. Brett, R. Anderson, A. Hahn, A.M. Innes, O. Suchowersky, M.B. Mets, G. Nürnberg, D.R. McLeod, H. Thiele, D. Waggoner, J. Altmüller, K.M. Boycott, B. Schoser, P. Nürnberg, C. Ober, R. Heller, J.S. Parboosingh, B. Wollnik, M. Sacher, R.E. Lamont, Recessive TRAPPC11 mutations cause a disease spectrum of limb girdle muscular dystrophy and myopathy with movement disorder and intellectual disability, Jul 11 2013. Am. J. Hum. Genet. 93 (1) 181–190, http://dx.doi.org/10.1016/j.ajhg.2013.05.028.
[34] W.C. Liang, W. Zhu, S. Mitsuhashi, S. Noguchi, M. Sacher, M. Ogawa, H.H. Shih, Y.J. Jong, I. Nishino, Congenital muscular dystrophy with fatty liver and infantile-onset cataract caused by TRAPPC11 mutations: broadening of the phenotype, Aug 28 2015. Skelet. Muscle 5 29, http://dx.doi.org/10.1186/s13395-015-0056-4 (eCollection 2015).
[35] C. Vantaggiato, E. Clementi, M.T. Bassi, ZFYVE26/SPASTIZIN: a close link between complicated hereditary spastic paraparesis and autophagy, Feb 2014. Autophagy 10 (2) 374–375, http://dx.doi.org/10.4161/auto.27173.
[36] J.K. Fink, Hereditary spastic paraplegia: clinico-pathologic features and emerging molecular mechanisms, 2013. Acta Neuropathol. http://dx.doi.org/10.1007/s00401-013-1115-8.
[37] J.G. Ghosh, M.R. Estrada, J.I. Clark, Interactive domains for chaperone activity in the small heat shock protein, human alphaβ crystallin, 2005. Biochemistry 44 14854–14869, http://dx.doi.org/10.1021/bi0503910.
[38] J.G. Ghosh, S.A. Houck, J.I. Clark, Interactive domains in the molecular chaperone human αB crystallin modulate microtubule assembly and disassembly, 2007. PLoS One 2 e498, http://dx.doi.org/10.1371/journal.pone.0000498.
[39] S. Sacconi, L. Féasson, J.C. Antoine, C. Pécheux, R. Bernard, A.M. Cobo, A. Casarin, L. Salviati, C. Desnuelle, A. Urtizberea, A novel CRYAB mutation resulting in multisystemic disease, 2012. Neuromuscul. Disord. 22 66–72, http://dx.doi.org/10.1371/journal.pone.0000498.
[40] I. Raju, E.C. Abraham, Mutants of human αB-crystallin cause enhanced protein aggregation and apoptosis in mammalian cells: influence of co-expression of HspB1, 2013. Biochem. Biophys. Res. Commun. 430 107–112, http://dx.doi.org/10.1016/j.bbrc.2012.11.051.
[41] H. Ecroyd, J.A. Carver, Crystallin proteins and amyloid fibrils, 2009. Cell. Mol. Life Sci. 66 62–81, http://dx.doi.org/10.1007/s00018-008-8327-4.
[42] M.D. Perng, S. Wen, P. van den Jssel, A.R. Prescott, R.A. Quinlan, Desmin aggregate formation by R120G αB-crystallin is caused by altered filament interactions and is dependent upon network status in cells, 2004. Mol. Biol. Cell 15 2335–2346, http://dx.doi.org/10.1091/mbc.E03-12-0893.
[43] J.P. Liu, R. Schlosser, W.Y. Ma, Z. Dong, H. Feng, L. Liu, X.Q. Huang, Y. Liu, D.W. Li, Human alphaA- and alphaB-crystallins prevent UVA-induced apoptosis through regulation of PKCalpha, RAF/MEK/ERK and AKT signaling pathways, 2004. Exp. Eye Res. 79 393–403, http://dx.doi.org/10.1016/j.exer.2004.06.015.
[44] N. Pasupuleti, S. Matsuyama, O. Voss, A.I. Doseff, K. Song, D. Danielpour, R.H. Nagaraj, The anti-apoptotic function of human αA-crystallin is directly related to its chaperone activity, 2010. Cell Death Dis. 1 e31, http://dx.doi.org/10.1038/cddis.2010.3.
[45] K.C. Kamradt, F. Chen, S. Sam, V.L. Cryns, The small heat shock protein alpha B-crystallin negatively regulates apoptosis during myogenic differentiation by inhibiting caspase-3 activation, 2002. J. Biol. Chem. 277 38731–38736, http://dx.doi.org/10.1074/jbc.M201770200.
[46] O. Ivanov, F. Chen, E.L. Wiley, A. Keswani, L.K. Diaz, H.C. Memmel, A. Rademaker, W.J. Gradishar, M. Morrow, S.A. Khan, αB-crystallin is a novel predictor of resistance to neoadjuvant chemotherapy in breast cancer, 2008. Breast Cancer Res. Treat. 111 411–417, http://dx.doi.org/10.1007/s10549-007-9796-0.
[47] J.G. Ghosh, A.K. Shenoy Jr., J.I. Clark, Interactions between important regulatory proteins and human alphaB crystallin, 2007. Biochemistry 46 6308–6317, http://dx.doi.org/10.1021/bi700149h.
[48] J.G. Ghosh, J.I. Clark, Insights into the domains required for dimerization and assembly of human alphaB crystallin, 2005. Protein Sci. 14 684–695, http://dx.doi.org/10.1110/ps.041152805.
[49] J.I. Clark, Self-assembly of protein aggregates in ageing disorders: the lens and cataract model, 2013. Philos. Trans. R. Soc. Lond. Ser. B Biol. Sci. 368 20120104, http://dx.doi.org/10.1098/rstb.2012.0104.
[50] J.I. Clark, Functional sequences in human alphaB crystallin, 2016. Biochim. Biophys. Acta 1860 (1 Pt B) 240–245, http://dx.doi.org/10.1016/j.bbagen.2015.08.014.
[51] R.M. Hussein, I.J. Benjamin, H.H. Kampinga, Rescue of αB-crystallin (HSPB5) mutants associated protein aggregation by co-expression of HSPB5 partners, 2015. PLoS One 10 e0126761, http://dx.doi.org/10.1371/journal.pone.0126761.
[52] D.G. McArthur, T.A. Manolio, D.P. Dimmock, H.L. Rehm, J. Shendure, G.R. Abecasis, D.R. Adams, R.B. Altman, S.E. Antonarakis, E.A. Ashley, J.C. Barrett, L.G. Biesecker, D.F. Conrad, G.M. Cooper, N.J. Cox, M.J. Daly, M.B. Gerstein, D.B. Goldstein, J.N. Hirschhorn, S.M. Leal, L.A. Pennacchio, J.A. Stamatoyannopoulos, S.R. Sunyaev, D. Valle, B.F. Voight, W. Winckler, C. Gunter, Guidelines for investigating causality of sequence variants inhuman disease, 2014. Nature 508 (204) 469–476, http://dx.doi.org/10.1038/nature13127.